Journal of
Mechanics of
Materials and Structures

CLASSICAL AND MIXED ADVANCED MODELS FOR SANDWICH PLATES EMBEDDING FUNCTIONALLY GRADED CORES

Salvatore Brischetto

Volume 4, Nº 1 January 2009

mathematical sciences publishers

JOURNAL OF MECHANICS OF MATERIALS AND STRUCTURES
Vol. 4, No. 1, 2009

CLASSICAL AND MIXED ADVANCED MODELS FOR SANDWICH PLATES EMBEDDING FUNCTIONALLY GRADED CORES

SALVATORE BRISCHETTO

This paper analyzes the bending response of several sandwich plates with a functionally graded core, using advanced equivalent single layer (ESL) and layerwise (LW) models with linear to fourth-order expansion in the thickness direction. The functionally graded properties of the core have been approximated by means of Legendre polynomials. The ESL and LW theories have been developed according to the *principle of virtual displacements* and *Reissner's mixed variational theorem*; in the latter case, both displacements and transverse shear/normal stresses have been assumed as primary variables. Closed-form solutions for simply supported sandwich plates loaded by a transverse distribution of harmonic pressure are discussed. Various assessments have been made of the proposed theories with respect to the available results. Our obtained results show that, depending on the chosen functionally graded core, the use of advanced models may turn out to be mandatory with respect to classical theories (for example, first-order shear deformation theory). It has been shown that the use of a core in functionally graded material can offer some advantages with respect to the classical cores that have been widely employed in open literature. A benchmark has been proposed which consists of a sandwich plate with two isotropic faces (ceramic and metallic) and various functionally graded cores. That benchmark could be useful in assessing future refined computational models.

1. Introduction

Functionally graded materials (FGMs) are composite materials made up of two or more constituent phases with a continuously variable composition. FGMs are usually associated with particulate composites where the volume fraction of particles varies in one or several directions. One of the advantages of a monotonous variation of volume fraction of the constituent phases is the elimination of stress discontinuity, which is often encountered in laminated composites and accordingly leads to the avoidance of delamination-related problems. FGMs present a number of advantages that make them attractive in potential future applications, such as a reduction of in-plane and transverse through-the-thickness stresses, an improved residual stress distribution, enhanced thermal properties, higher fracture toughness, and reduced stress intensity factors [Birman and Byrd 2007]. For these reasons, an accurate evaluation of displacements, strains, stresses, and vibrations can be fundamental in the design of such structures.

Several three-dimensional solutions are proposed in the literature for the case of simple problems in one-layered FGM structures. Among these, the three-dimensional elasticity solution proposed by Kashtalyan [2004] for a functionally graded simply supported plate subjected to transverse loading is of particular interest. Young's modulus of the plate is assumed to vary exponentially through the thickness

Keywords: functionally graded materials, sandwich plates with an FGM core, Carrera's unified formulation, classical models, mixed models, equivalent single layer theories, layerwise theories, Legendre polynomials.

and the Poisson's ratio is assumed to be constant. Reddy and Cheng [2001] propose a three-dimensional thermomechanical solution for simply supported functionally graded rectangular plates by means of an asymptotic method. The locally effective material properties are estimated by the scheme from [Mori and Tanaka 1973]. Vel and Batra [2002; 2003; 2004] give exact three-dimensional solutions for functionally graded rectangular plates in the case of mechanical and thermal loads on its top and/or bottom surfaces, time-dependent thermal loads, and free and forced vibrations.

Here are some classical and advanced two-dimensional models for these structures made up of one FGM layer: Zenkour [2006] presents the static response for a simply supported functionally graded rectangular plate subjected to a transverse load, where a generalized shear deformation theory is used and the material properties of the plate are assumed to be graded in the thickness direction, according to a simple power-law distribution in terms of the volume fractions of the constituents. Chi and Chung [2006] use the classical plate theory and Fourier series expansion to investigate an elastic, rectangular, and simply supported, FGM plate of medium thickness subjected to transverse loading. Ramirez et al. [2006] obtain a solution for an FGM plate by using a discrete layer theory in combination with the Ritz method in which the plate is divided into an arbitrary number of homogeneous and/or FGM layers. Two types of functionally graded materials are considered: an exponential variation of the mechanical properties through the thickness of the plate, and mechanical properties as a function of the fiber orientation, which varies quadratically through the laminate thickness. Another method used to analyze the static deformations of a simply supported functionally graded plate modeled by a third-order shear deformation theory is the use of the collocation multiquadric radial basis functions proposed by Ferreira et al. [2005]. As far as the dynamic analysis is concerned, Qian et al. [2004] investigate the free and forced vibrations of a thick rectangular functionally graded elastic plate using a higher-order shear and normal deformable plate theory and a meshless local Petrov–Galerkin method, Batra and Jin [2005] use first-order shear deformation theory (FSDT) coupled with the finite element method to study free vibrations of a functionally graded anisotropic rectangular plate with the objective of maximizing one of its first five natural frequencies. Nguyen et al. [2008] identify the transverse shear factor by means of energy equivalence for a one-layered FGM plate in the case of first-order shear deformation theory.

All the works mentioned above refer to the case of plates made up of one FGM layer, where the three-dimensional solutions represent very interesting reference solutions and the other two-dimensional models are valuable tools to investigate such problems. The main aim of the present paper is the use of FGMs in multilayer structures. These graded layers can be used as face sheets or as core and its employment can be very efficient to solve some problems usually connected to classical sandwich structures. /'Avila [2007] considers sandwich beams with a functionally graded core. The proposed failure mode model accurately predicts the failure mechanisms. The best performance is obtained when the core layer with the highest density is located right below the upper face-sheets. Cheng and Zhong [2007] consider a finite crack with constant length propagating in the functionally graded layer. The structure is a functionally graded strip between two dissimilar homogeneous layers. The importance of graded parameters in the dynamic fracture behavior is clearly demonstrated. Considering a functionally graded transition zone between a hard TiC coating and a WC-Co substrate, Dahan et al. [2001] show that the critical load and the wear resistance depend on the concentration profile within the transition layer. The Ti-rich profiles displayed the highest critical load and the lowest wear rate. The transition response of a crack embedded in a functionally graded material layer sandwiched between two dissimilar elastic

layers is analyzed under antiplane shear impact loads by Li and Fan [2007]. The effects of crack position, material properties, and the FGM layer thickness are investigated. Xia and Shen [2008] use a high-order shear deformation theory to investigate small and large amplitude vibrations of a compressively and thermally postbuckled sandwich plate with FGM face sheets. When the volume fraction index increases, the fundamental frequency increases in the prebuckling region, but decreases in the postbuckling region. The resulting fracture behavior under impact loading conditions in sandwich structures comprising an FGM core has been illustrated by Kirugulige et al. [2005]. These results show a significant reduction in stress intensification in the presence of compositional gradients compared to conventional constructions. The results concerning a sandwich with a homogeneous core and FGM face sheets by Shen and Li [2008] show that the thermal buckling load is modified when using FGM faces. Zhao et al. [2008] investigate the effects of FGM coatings on the thermal shock resistance of a sandwich plate with functionally graded coatings. A two-dimensional solution for the bending analysis, buckling study, and free vibrations of a functionally graded sandwich plate is the sinusoidal shear deformation plate theory by Zenkour [2005a; 2005b]. The exact thermoelasticity solution of Shodja et al. [2007] analyzes a thick composite structure consisting of homogeneous and functionally graded layers; stress concentration effects are eliminated and interfacial shear stresses are reduced. The three-dimensional finite element simulations by Etemadi et al. [2008] analyze low velocity impact behavior of sandwich beams with an FGM core. For sandwich beams with functionally graded cores, the maximum contact force increases and the maximum strain decreases compared to those of sandwich beams with a homogeneous core. Anderson [2003] developed an analytical three-dimensional elasticity solution method for a sandwich composite with a functionally graded core subjected to a transverse loading by a rigid spherical indentor. The effects of FGM face sheets and a homogeneous core, or homogeneous face sheets and an FGM core on the free vibrations of sandwich plates with simply supported or clamped edges, are analyzed by Li et al. [2008] by means of a three dimensional linear elasticity theory. The benefits of the use of an FGM core in a sandwich plate for the stresses are analyzed by Kashtalyan and Menshykova [2009] using a three-dimensional solution.

In conclusion, the use of FGM face sheets and/or core in sandwich structures can be very useful to contrast failure mechanisms and crack propagations, to increase critical and buckling loads, to decrease the wear rate, the stress concentration effects and the interfacial shear stresses, and to improve thermal shock resistance. The importance of new accurate plate theories to investigate such types of sandwich structures, as done in [Zhu and Sankar 2007] in the case of a thermal protection system panel with a functionally graded foam core, is therefore clear.

In the present paper, in order to obtain advanced two-dimensional models for sandwich structures with FGM layers, Carrera's unified formulation [1995; 2002], known as CUF, has been extended to materials with properties that are functionally graded through the thickness direction. This extension was made for the classical advanced models in [Carrera et al. 2008] and for the mixed ones in [Brischetto and Carrera 2008]. In the first case, the principle of virtual displacements (PVD) was used, while in the second paper, Reissner's mixed variational theorem (RMVT) was employed to model both displacements and transverse shear/ normal stresses. The classical and mixed advanced hierarchical models presented in these two papers were developed for multilayer FGM plates. Applications were only made for single-layered FGM structures. In the present paper, considering sandwich plates with an FGM core, the models obtained in [Carrera et al. 2008] and [Brischetto and Carrera 2008] are validated for multilayer FGM plates. For material properties, only spatial dependence has been considered. These properties have

been considered independent of temperature; the dependence on temperature will be added in future work, where the heat conduction problem will be accounted for. The most important features about the extension of CUF to FGMs have been discussed in Section 2, then Section 3 introduces the employed kinematic models. Section 4 deals with the results and discussion, and the conclusions are given in Section 5.

2. Extension of CUF to FGMs

The application of a two dimensional method for plates allows the unknown variables to be expressed in a set of thickness functions that only depend on the thickness coordinate z and the correspondent variable which depends on the in-plane coordinates (x, y).

CUF is a technique which handles a large variety of plate/shell modelings in a unified manner [Carrera 1995; 2002]. According to CUF, the governing equations are written in terms of a few *fundamental nuclei* which do not formally depend on

- the order of expansion N used in the z-direction, and
- the variables description: layerwise (LW) or equivalent single layer (ESL).

The generic variable $\boldsymbol{a}(x, y, z)$, for instance a displacement, and its variation $\delta\boldsymbol{a}(x, y, z)$ are therefore written according to the general expansion

$$\boldsymbol{a}(x, y, z) = F_\tau(z)\boldsymbol{a}_\tau(x, y), \quad \delta\boldsymbol{a}(x, y, z) = F_s(z)\delta\boldsymbol{a}_s(x, y) \quad \text{for } \tau, s = 1, \ldots, N, \tag{1}$$

where the bold letters denote arrays, (x,y) are the in-plane coordinates and z the thickness one, and $F_\tau(z)$ and $F_s(z)$ are thickness functions. The summation convention is assumed with repeated indexes τ and s. The order of expansion N goes from first to fourth order, and depending on the used thickness functions $F(z)$, one model could be ESL when the variable is assumed for the whole multilayer and LW when the variable is considered independent in each layer.

A model for the analysis of FGM plates must accurately describe the continuous variations of the material characteristics (mechanical, thermal, or electric) along the thickness. The present section focuses on the procedure that allows the CUF to be expanded to the analysis of FGM layers. These layers could be single or embedded in other classical and/or FGM layers. For the FGM layers, Legendre polynomials have been used to approximate the elastic coefficients in the thickness z.

The variation of the material characteristics is usually given in terms of exponential and/or polynomial functions applied directly to engineering constants such as Young's moduli E_i, shear moduli G_{ij} and/or Poisson's ratio ν_{ij}, or directly to material stiffnesses C_{ij} with $i, j = 1, 6$. Since a relation between the engineering constants and the material stiffnesses holds in each point of the plate, only the second case can actually be treated. The variation of the stiffness matrix is generally given by multiplying it by a function of z

$$\boldsymbol{C}(z) = \boldsymbol{C}_0 * g(z), \tag{2}$$

where $\boldsymbol{C}_0$ is the reference stiffness matrix and $g(z)$ gives the variation along z. By applying the ideas behind the CUF, the following expansion is made

$$\boldsymbol{C}(z) = F_b(z)\boldsymbol{C}_b + F_\gamma(z)\boldsymbol{C}_\gamma + F_t(z)\boldsymbol{C}_t = F_r\boldsymbol{C}_r, \tag{3}$$

where the *thickness functions* F_γ are the same that will be used for the LW expansion in the next section

$$F_t = \frac{P_0 + P_1}{2}, \quad F_b = \frac{P_0 - P_1}{2}, \quad F_\gamma = P_\gamma - P_{\gamma-2} \quad \gamma = 2, \ldots, N_r, \tag{4}$$

where $P_j = P_j(\zeta_k)$ is the Legendre polynomial of j-th order defined in the domain $-1 \leq \zeta_k \leq 1$.

The actual $\boldsymbol{C}$ is then recovered as a weighted summation on the terms $\boldsymbol{C}_r$. The weights are given by the thickness functions F_r. The order of the expansion can be arbitrarily chosen. Due to the usual complicated laws used for $g(z)$ in the open literature, the expansion has been in this work extended to $N_r = 10$. Anyway, when a simple polynomial $g(z)$ is applied lower values of N_r could be used.

The procedure to include the varying stiffnesses in the model requires to compute the $\boldsymbol{C}_r$ matrices. This task can be accomplished solving for each component C_{ijr} a simple algebraic system of order N_r. After that the actual values of C at N_r different locations along the thickness $(z_1, \ldots, z_{N_r})$ have been calculated, leading to the formula

$$\begin{bmatrix} C_{ij}(z_1) \\ \vdots \\ C_{ij}(z_{N_r}) \end{bmatrix} = \begin{bmatrix} F_b(z_1) & \cdots & F_\gamma(z_1) & \cdots & F_t(z_1) \\ \vdots & & \vdots & & \vdots \\ F_b(z_{N_r}) & \cdots & F_\gamma(z_{N_r}) & \cdots & F_t(z_{N_r}) \end{bmatrix} \begin{bmatrix} C_{ijb} \\ \vdots \\ C_{ijr} \\ \vdots \\ C_{ijt} \end{bmatrix}. \tag{5}$$

In the case of classical layers with constant material properties the formula in Equation (3) is not considered and the elastic coefficients are constant in the rigidity matrices.

A detailed description of the CUF extended to FGMs is reported in [Carrera et al. 2008] for the PVD (only the displacements are considered as primary variables) and in [Brischetto and Carrera 2008] for the RMVT (both displacements and transverse shear/normal stresses as primary variables). Further details regarding the assembly procedure (expansion in z for the primary variables and material properties, multilayer assembly procedure) and the governing equations can be found in these same two papers.

3. Description of kinematics

The proposed two-dimensional models have been coded according to the CUF. Details can be found in previous authors' works [Carrera1995; 2002; Brischetto and Carrera 2008; Carrera et al. 2008]. In order to explore how the various kinematic assumptions can affect the response of typical two-dimensional structures, a large variety of plates/shells theories have been considered here.

Plates of constant thickness h are considered. The geometry and reference system are shown in Figure 1. The displacement components u_x, u_y, and u_z are measured with respect to the x, y, and z axes. The latter axis denotes the trough-the-thickness direction. Ω is the plate reference surface. Plain-stress/plain-strain conditions have been assumed according to what indicated in the paper concerning the Poisson's locking phenomena for plates [Carrera and Brischetto 2008].

Higher-order theories. Higher-order theories (HOTs) consider the same order of expansion in the thickness direction for the three displacements components (including the transverse one). These theories are obtained in the ESL overview.

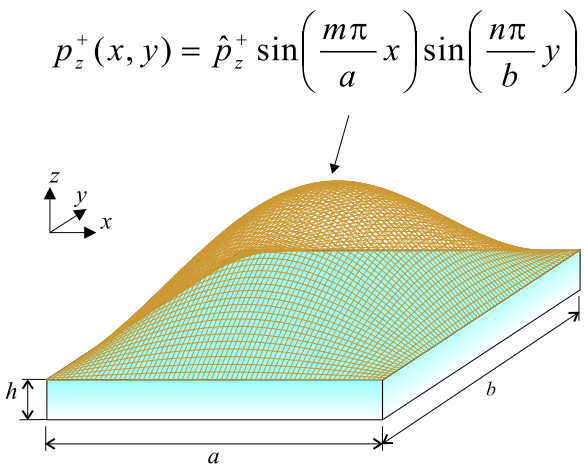

Figure 1. Notations and load configuration for the plates considered.

HOTs including transverse normal strains. Higher-order terms can be introduced in the kinematic assumptions in order to obtain refinements of classical lamination theory (CLT) and FSDT models

$$u_\tau(x, y, z) = u_{0\tau}(x, y) + z^i u_{i\tau}(x, y) \quad \text{with } \tau = x, y, z \text{ and } i = 1, N. \tag{6}$$

The summation convention for the repeated indexes has been adopted. N is the order of expansion, which is taken as a free parameter. In the numerical investigation N is considered to be as low as 1 and as high as 4. According to the acronym system developed within CUF, the related theories are named ED1–ED4. The letter E denotes that the kinematic is preserved for the whole layers, as in the ESL approach, while D denotes that only displacement unknowns are used and the last number states the through-the-thickness expansion order.

HOTs including zigzag effects. The EDN models are not able to describe the discontinuity of the first derivative with correspondence to the layer interfaces, known as the zigzag effects [Carrera 2003] and peculiar of laminates mechanics. It can be introduced via the Murakami's zigzag function (MZZF) [Murakami 1986], which was proposed in the framework of RMVT applications. The dimensionless layer coordinate $\zeta_k = (2z_k)/h_k$ is further introduced, being h_k the thickness of the k-th layer and z_k the layer thickness coordinate. MZZF is defined according to the formula

$$\text{MZZF} = (-1)^k \zeta_k. \tag{7}$$

MZZF has the following properties: it is piecewise linear function of the layer coordinate z_k, it has unit amplitude for the whole layers, and its slope takes opposite sign between two-adjacent layers, since its amplitude layer is independent of thickness. The displacement field accounting for MZZF takes the form

$$u_\tau(x, y, z) = u(x, y)_{0\tau} + z^r u(x, y)_{r\tau} + (-1)^k \zeta_k u(x, y)_{Z\tau} \quad \text{with } \tau = x, y, z \text{ and } r = 1, 2, \ldots, N-1. \tag{8}$$

Subscript Z refers to the introduced zigzag term. Higher-order distributions in the z-direction are introduced by polynomials of degree r. Modifications of EDN directed to include MZZF are denoted EDZN.

The classical theories. The classical theory CLT, based on assumptions made by Cauchy [1828], Poisson [1829], and Kirchhoff [1850], discards transverse shear and through-the-thickness deformations. The displacement model related to CLT can be written in the form

$$u_\tau(x, y, z) = u_{0\tau}(x, y) - z\frac{\partial u_{0z}(x, y)}{\partial \tau} \quad \text{with } \tau = x, y \text{ and } u_z(x, y, z) = u_{0z}(x, y), \tag{9}$$

stating that the section remain plane and orthogonal to the plate reference surface Ω. Here u_0 denotes the displacement value relative to the reference surface Ω. Transverse shear stresses are discarded by CLT.

Transverse shear deformation can be introduced according to the Reissner–Mindlin kinematic assumptions [Reissner 1945; Mindlin 1951]:

$$u_\tau(x, y, z) = u_{0\tau}(x, y) + z u_{1\tau}(x, y) \quad \text{with } \tau = x, y \text{ and } u_z(x, y, z) = u_{0z}(x, y). \tag{10}$$

This theory is also called FSDT. Transverse shear stresses show a priori constant piecewise distribution. FSDT can be obtained from ED1 by considering a constant transverse displacement through the thickness. CLT is obtained from FSDT considering an infinite shear correction factor. In both CLT and FSDT, the Poisson locking phenomenon is contrasted by means of the plane-stress conditions, as indicated in [Carrera and Brischetto 2008]. In the proposed analysis of FGM structures, the shear correction factor has not been used for the correction of FSDT because the well-known value $\chi = 5/6$ is calculated for a homogeneous material. The shear correction factor for a general laminate depends on lamina properties and lamination scheme [Reddy 2004].

Layerwise theories. Multilayered plates can be analyzed by kinematic assumptions which are independent in each layer. Following Reddy [2004] these approaches are called here LW theories.

The LW description yields, thus, displacement variables that are independent in each layer. The Taylor expansion of the thickness, adopted in the previous paragraphs for ESL cases, is not convenient for LW description. Displacement interlaminar continuity can be imposed more conveniently by employing interface values as unknown variables. The LW description assumes the form

$$u^k_\tau = F_t\, u^k_{\tau t} + F_b\, u^k_{\tau b} + F_r\, u^k_{\tau r} \quad \text{with } \tau = x, y, z, \quad r = 2, 3, \ldots, N, \quad k = 1, 2, \ldots, N_l. \tag{11}$$

Subscript t and b denote values related to the top and the bottom of layer, respectively. The thickness functions $F_\tau(\zeta_k)$ have been defined by

$$F_t = \frac{P_0 + P_1}{2}, \quad F_b = \frac{P_0 - P_1}{2}, \quad F_r = P_r - P_{r-2}, \quad r = 2, 3, \ldots, N, \tag{12}$$

in which $P_j = P_j(\zeta_k)$ is the j-th order Legendre polynomial defined for $-1 \le \zeta_k \le 1$. In the numerical investigations the maximum order is four, and the relevant polynomials are

$$P_0 = 1, \quad P_1 = \zeta_k, \quad P_2 = (3\zeta_k^2 - 1)/2, \quad P_3 = \frac{5\zeta_k^3}{2} - \frac{3\zeta_k}{2}, \quad P_4 = \frac{35\zeta_k^4}{8} - \frac{15\zeta_k^2}{4} + \frac{3}{8}. \tag{13}$$

The preceding functions have the following interesting properties:

$$\text{when } \zeta_k = 1\text{: } F_t = 1,\ F_b = 0,\ F_r = 0; \quad \text{when } \zeta_k = -1\text{: } F_t = 0,\ F_b = 1,\ F_r = 0. \tag{14}$$

The top and bottom values have been used as unknown variables. The interlaminar compatibility of displacement can therefore be easily linked:

$$u^k_{\tau t} = u^{(k+1)}_{\tau b}, \quad k = 1, N_l - 1. \tag{15}$$

The acronyms for these theories are LD1–LD4, the L standing for LW.

Mixed theories based on Reissner's mixed variational theorem. The kinematics described previously is not able to furnish interlaminar continuity of transverse shear and normal stresses at the interfaces between two adjacent layers in the case of multilayer structures. RMVT [Reissner 1984] offers the possibility to fulfil a priori the interlaminar continuity. Both displacements and transverse shear/normal stresses can be assumed within the RMVT framework as primary variables.

Layerwise mixed theories. In the LW case the displacement model in (11) is also used for the transverse shear/normal stresses:

$$\sigma^k_{\tau z} = F_t \sigma^k_{\tau z_t} + F_b \sigma^k_{\tau z_b} + F_r \sigma^k_{\tau z_r} \quad \text{with } \tau = x, y, z, \quad r = 2, 3, \ldots, N, \quad k = 1, 2, \ldots, N_l. \tag{16}$$

The interlaminar transverse shear and normal stresses continuity can be, therefore, easily linked:

$$\sigma^k_{\tau z_t} = \sigma^{(k+1)}_{\tau z_b} \quad \text{with } \tau = x, y, z, \quad k = 1, N_l - 1. \tag{17}$$

These models are denoted as LM1–LM4, where M means mixed models based on RMVT.

Equivalent single layer mixed theories. Mixed theories along with an ESL description can be formulated referring to the displacement model in (6) and the LW stress assumptions in (16). These are referred to as EM1–EM4. The theories accounting for the zigzag shape of the displacements are indicated as EMZ1–EMZ3. A further letter C could be added in the acronyms to emphasize the continuity of the transverse shear/normal stresses.

4. Results and discussion

All the examples presented in this section consider a simply supported square plate with a bisinusoidal mechanical load applied to the top surface; see Figure 1. The applied load is

$$p_z(x, y) = \bar{p}_z \sin\left(\frac{m\pi}{a}x\right) \sin\left(\frac{n\pi}{b}y\right), \tag{18}$$

where a and b are the plate dimensions, x and y are the in-plane coordinates and z is the thickness coordinate. The load amplitude is $\bar{p}_z = 1.0\,\text{Pa}$ and the wavelengths in the x and y directions are $m = n = 1$.

Assessment 1: one-layered no-FGM plate. The plate is made of aluminum Al2024 with Young's modulus $E = 73\,\text{GPa}$ and Poisson's ratio $\nu = 0.34$. The global thickness is $h = 0.001\,\text{m}$ and the thickness ratio is $a/h = 10$. The three-dimensional solution for the dimensionless transverse displacement $\bar{w}$ considered in the middle of the plate is given in [Carrera and Brischetto 2008]. The transverse normal stress σ_{zz} at the top is given by the loading conditions. Table 1 compares a classical theory (FSDT) and advanced classical and mixed models with the three-dimensional solution, to demonstrating how the models for functionally graded materials can degenerate into models for materials with constant properties through thickness z. The fictitious layers (Figure 2) have been introduced to validate the multilayer assembly

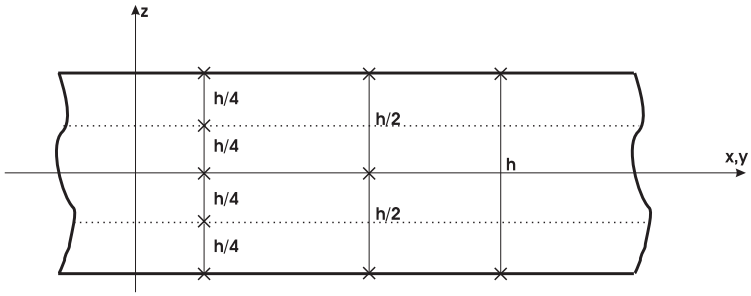

Figure 2. Assessment 1: Isotropic square plate with fictitious layers.

	One layer		Two layers		Four layers	
	$\bar{w}(0)$	$\sigma_{zz}(h/2)$	$\bar{w}(0)$	$\sigma_{zz}(h/2)$	$\bar{w}(0)$	$\sigma_{zz}(h/2)$
3D	2.8655	1.0000	2.8655	1.0000	2.8655	1.0000
FSDT	2.7238	1.5659	2.7238	1.5659	2.7238	1.5659
ED4	2.8655	1.0001	2.8655	1.0001	2.8655	1.0001
EM4	2.8655	1.0001	2.8655	1.0001	2.8655	1.0001
LD4	2.8655	1.0001	2.8655	1.0001	2.8655	1.0000
LM4	2.8655	1.0001	2.8655	1.0000	2.8655	1.0000

Table 1. Assessment 1: Isotropic square plate with thickness ratio $a/h = 10$. The 3D case corresponds to [Carrera and Brischetto 2008]. Results for one layer, two and four fictitious layers. The dimensionless transverse displacement is $\bar{w} = 100Eh^3u_z/(\bar{p}_z a^4)$.

procedure. Though a shear correction factor $\chi = 5/6$ could be used for FSDT in case of homogeneous and isotropic plates, $\chi = 1$ has been employed to be consistent with the case of FGM structures.

Assessment 2: one-layered FGM plate. The considered plate is one-layered with Young's modulus $E(z)$ changing in the thickness direction z, according to Zenkour's formula [2006]

$$E(z) = E_m + (E_c - E_m)\left(\frac{2z+h}{2h}\right)^{\kappa}. \tag{19}$$

The plate is completely metallic at the bottom ($E_m = 70\,\text{GPa}$) and completely ceramic at the top ($E_c = 380\,\text{GPa}$). A constant Poisson ratio $\nu = 0.3$ and a thickness ratio $a/h = 10$ are considered. Varying the thickness coordinate z from $-h/2$ to $h/2$, Young's modulus changes with continuity, as illustrated in Figure 3, where the exponential κ varies from 1 to 10. The global thickness is $h = 0.1\,\text{m}$. A detailed investigation was made in [Carrera et al. 2008] for PVD models and in [Brischetto and Carrera 2008] for RMVT models. The FSDT model is compared in Table 2 with some advanced ones ($\kappa = 1$), with the solution from [Zenkour 2006] (a generalized shear deformation model), and with a discrete layer quasi-three-dimensional solution previously presented in [Carrera et al. 2008]. The fictitious layers, as illustrated in Figure 4, have been considered to demonstrate that the present models are able to carry out the multilayer FGM assembly procedure.

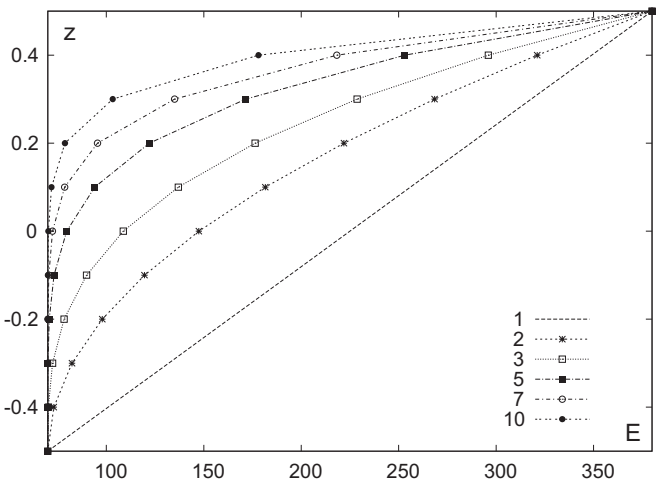

Figure 3. Young's modulus $E(z)$ versus z for different values of the parameter κ considered in the Zenkour's formula (19).

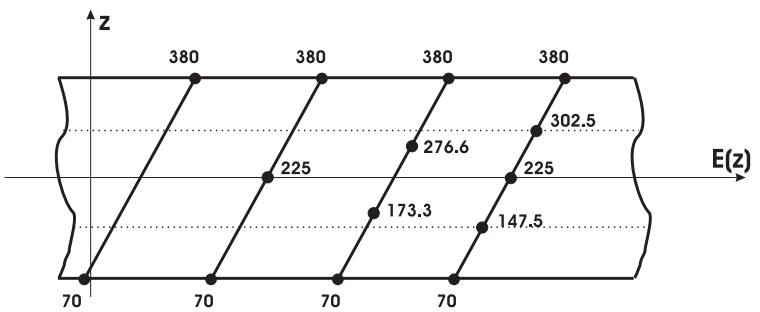

Figure 4. Assessment 2: Functionally graded plate with linear ($\kappa = 1$) Zenkour's law [2006] and fictitious layers.

	One $\bar{w}(0)$	Two $\bar{w}(0)$	Three $\bar{w}(0)$	Four $\bar{w}(0)$
Z	0.5889	0.5889	0.5889	0.5889
CBR	0.5875	0.5875	0.5875	0.5875
FSDT	0.4812	0.4812	0.4812	0.4812
ED4	0.5875	0.5875	0.5875	0.5875
EM4	0.5875	0.5875	0.5875	0.5875
LD4	0.5875	0.5875	0.5875	0.5875
LM4	0.5875	0.5875	0.5875	0.5875

Table 2. Assessment 2: Functionally graded square plate with thickness ratio $a/h = 10$ and exponential $\kappa = 1$ for Zenkour's formula [2006] (row marked Z). CBR stands for [Carrera et al. 2008]. Results are shown for one layer and for two, three and four fictitious layers. The dimensionless transverse displacement is $\bar{w} = 10E_c h^3 u_z/(\bar{p}_z a^4)$.

Assessment 3: sandwich FGM plate. A further validation for the employed ESL and LW models, based on PVD and RMVT, is made with the three-dimensional solution proposed by Kashtalyan and Menshykova [2009] for the case of a three-layered plate with a core in FGM; see Figure 5. The global thickness of the plate is $h_0 = 2h$ where h and $-h$ represent the top and bottom coordinates of the plate, respectively. h_c and $-h_c$ are the coordinates of the bottom fourth layer and the top first layer, respectively. The global thickness of the core is $2h_c$. The plate has a global thickness $h_0 = 1.0\,\text{m}$, the thickness of

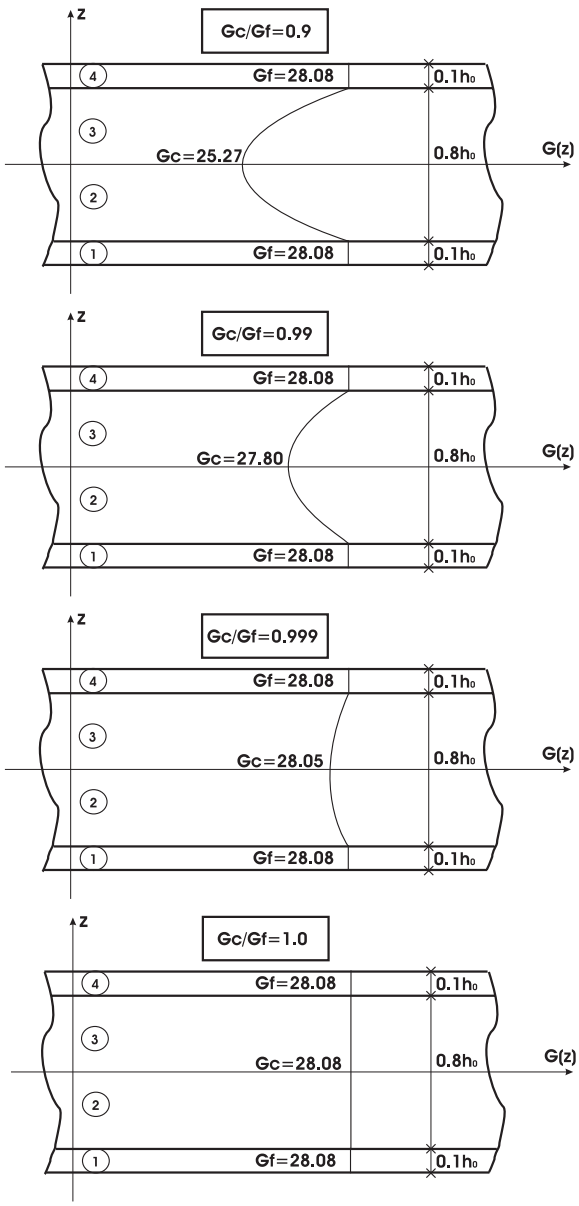

Figure 5. Assessment 3: Examples of different sandwich plates with core in FGM, following [Kashtalyan and Menshykova 2009].

the two faces is $h_f = 0.1h_0$, and the thickness of the core is $2h_c = 0.8h_0$. The considered thickness ratio is $a/h_0 = 3$. The reference Young's modulus is $E_0 = 73\,\text{GPa}$ with Poisson's ratio $\nu = 0.3$, and the two faces consequently have a constant shear modulus $G_f = G_0 = 28.08\,\text{GPa}$ (layers 1 and 4). The core can be divided into parts 2 and 3. The value of the shear modulus in the middle reference surface is indicated with G_c. In layer 2, the exponential law for the shear modulus is $G(z) = G_0 \exp[-\gamma\,(z/h_c + 1)]$ with $h_c = 0.4\,\text{m}$ and $-0.4 \le z \le 0$. For layer 3, the exponential law is $G(z) = G_0 \exp[\gamma\,(z/h_c - 1)]$ with $h_c = 0.4\,\text{m}$ and $0 \le z \le 0.4$. Four different cases will be considered, as illustrated in Figure 5, that correspond to four different shear modulus ratios G_c/G_f (0.9, 0.99, 0.999, 1.0), which means values of the exponential γ equal to 0.105360, 0.010050, 0.001000 and 0.0, respectively. The case $G_c/G_f = 1.0$ means a three-layered plate with the same classical material. Table 3 (page 26) considers the dimensionless transverse displacement $\bar{w}$ in the middle for different values of G_c/G_f; the transverse normal stress σ_{zz} at the top and bottom of the plate is investigated in Table 4. The three-dimensional reference solution is given by Kashtalyan and Menshykova [2009]. For the displacements, when the shear modulus ratio is close to 1.0, both LW and ESL models are able to give the three-dimensional response, but the requested order of expansion in z is lower for the LW models. In the case of $G_c/G_f = 0.9$, the use of LW models and higher orders of expansion is mandatory. The addition of MZZF [Murakami 1986] to ESL models is not so effective as in the case of classical sandwich structures where the typical zigzag form of the displacement is observable. The comments made for the PVD models in Table 3 are confirmed for the RMVT models on the right-hand side of the same table. To obtain the correct values of the stresses, LW and higher orders of expansions are requested, as suggested by Table 4.

The advantage of RMVT models is clearly demonstrated in the case of LW models with lower orders of expansions and in the case of ESL theories. These conclusions become much clearer if we consider Figures 6 and 7. In Figure 6, where the displacements are plotted along the thickness, it is evident that the use of a higher order of expansion is fundamental. In Figure 7, in the case of transverse shear/normal stresses σ_{xz} and σ_{zz}, for a shear modulus ratio $G_c/G_f = 0.9$, the use of RMVT models is mandatory.

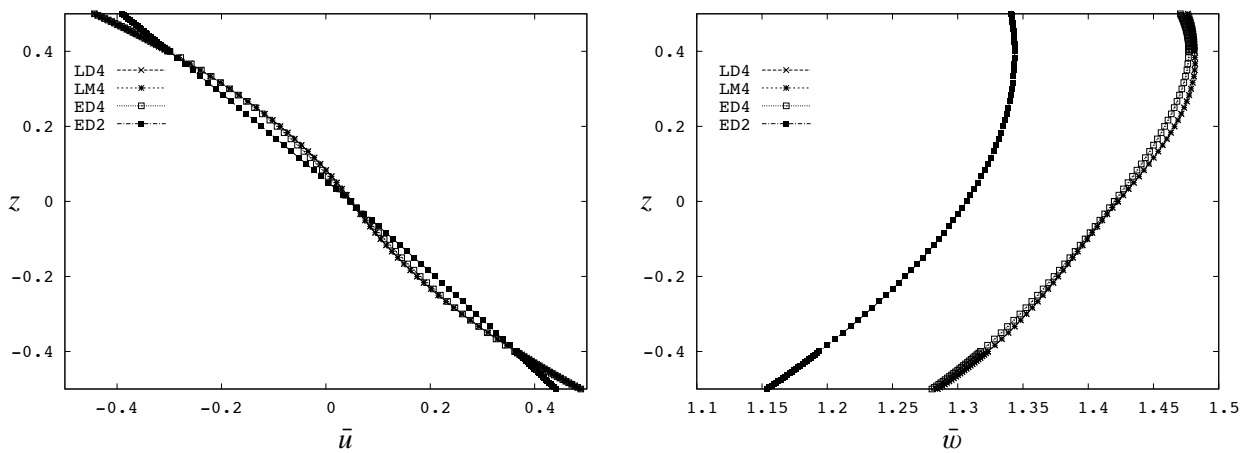

Figure 6. Assessment 3: Displacements $\bar{u} = G_0 u_x/(\bar{p}_z h_0)$ and $\bar{w} = G_0 u_z/(\bar{p}_z h_0)$ vs. z, for the sandwich plate with core in FGM proposed in [Kashtalyan and Menshykova 2009]. The shear modulus is $G_c/G_f = 0.9$.

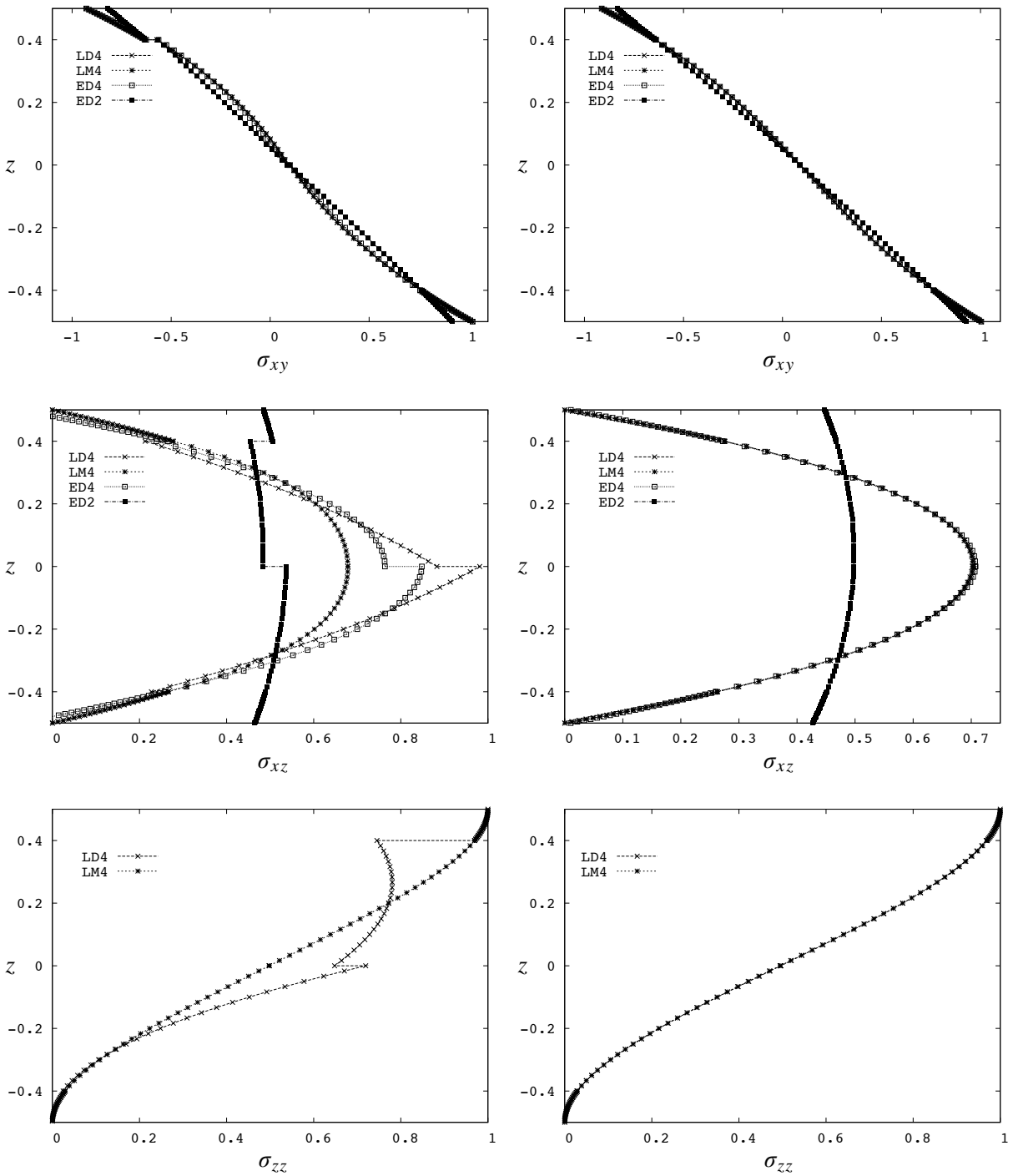

Figure 7. Assessment 3: Sandwich plates with core in FGM according to the solution and formula from [Kashtalyan and Menshykova 2009]. $G_c/G_f = 0.9$ (left column) and $G_c/G_f = 0.999$ (right column). σ_{xy}, σ_{xz} and σ_{zz} versus z.

	G_c/G_f	0.9	0.99	0.999	1.0
	3D	1.4227	1.3500	1.3433	1.3430
ESL theories	FSDT	1.1924	1.1714	1.1690	1.1687
	ED1	1.1924	1.1714	1.1690	1.1687
	ED2	1.3067	1.2820	1.2792	1.2789
	ED3	1.4223	1.3518	1.3453	1.3446
	ED4	1.4199	1.3496	1.3432	1.3424
ESL + MZZF	EDZ1	1.1999	1.1796	1.1772	1.1769
	EDZ2	1.3027	1.2728	1.2750	1.2747
	EDZ3	1.4179	1.3472	1.3407	1.3400
LW theories	LD1	1.3584	1.3190	1.3149	1.3144
	LD2	1.4213	1.3476	1.3413	1.3406
	LD3	1.4227	1.3495	1.3432	1.3425
	LD4	1.4227	1.3496	1.3432	1.3426

G_c/G_f	0.9	0.99	0.999	1.0
3D	1.4227	1.3500	1.3433	1.3430
EM1	1.1936	1.1714	1.1690	1.1687
EM2	1.3069	1.2820	1.2792	1.2789
EM3	1.4224	1.3518	1.3453	1.3446
EM4	1.4200	1.3496	1.3432	1.3424
EMZ1	1.2022	1.1808	1.1783	1.1781
EMZ2	1.3023	1.2774	1.2746	1.2742
EMZ3	1.4176	1.3470	1.3405	1.3398
LM1	1.4029	1.3498	1.3445	1.3439
LM2	1.4190	1.3464	1.3402	1.3395
LM3	1.4228	1.3498	1.3435	1.3428
LM4	1.4227	1.3495	1.3432	1.3425

Table 3. Assessment 3: Sandwich plate with core in functionally graded material and two external isotropic faces. The three-dimensional solution is from [Kashtalyan and Menshykova 2009]. The thickness ratio is $a/h = 3$ and the dimensionless transverse displacement is $\bar{w} = G_0 u_z/(\bar{p}_z h_0)$ evaluated at $z = 0$. Left: classical model and advanced models based on PVD; right: advanced models based on RMVT.

	$\sigma_{zz}(h/2)$				$\sigma_{zz}(-h/2)$			
G_c/G_f	0.9	0.99	0.999	1.0	0.9	0.99	0.999	1.0
L.C.	1.0000	1.0000	1.0000	1.0000	0.0000	0.0000	0.0000	0.0000
FSDT	1.1536	1.1709	1.1723	1.1724	−1.536	−1.1709	−1.723	−1.1724
ED3	1.1766	1.2226	1.2266	1.2271	−0.3439	−0.2374	−0.2278	−0.2267
ED4	0.9060	0.9940	1.0026	1.0035	−0.0738	−0.0043	0.0016	0.0023
EDZ1	1.2727	1.2496	1.2473	1.2471	−0.2456	−0.2852	−0.2894	−0.2899
EDZ3	0.9060	0.9671	0.9726	0.9732	−0.0738	0.0219	0.0304	0.0313
LD2	1.0119	1.0119	1.0119	1.0119	−0.0105	−0.0104	−0.0104	−0.0104
LD4	1.0000	1.0000	1.0000	1.0000	0.0000	0.0000	0.0000	0.0000
EM3	1.1453	1.2196	1.2263	1.2271	−0.3444	−0.2374	−0.2278	−0.2267
EM4	0.9319	0.9968	1.0028	1.0035	−0.0732	−0.0043	0.0016	0.0023
EMZ1	1.4291	1.3544	1.3472	1.3464	−0.3527	−0.3837	−0.3866	−0.3869
EMZ3	1.0023	1.0334	1.0363	1.0366	−0.1435	−0.0419	−0.0328	−0.0318
LM2	1.0046	1.0071	1.0067	1.0066	−0.0130	0.0036	0.0043	0.0043
LM4	1.0002	1.0001	1.0001	1.0000	0.0000	0.0000	0.0000	0.0000

Table 4. Assessment 3: Values of σ_{zz} on plate surface for the same setup as in Table 3. L.C. means loading condition (expected value of σ_{zz}).

The stresses obtained a priori are in fact continuous in the thickness z direction. The use of ESL models is not effective for the evaluation of such stresses for either cases of $G_c/G_f = 0.9$ or $G_c/G_f = 0.999$. If we consider a value of G_c/G_f close to 1.0, the use of PVD models is sufficient, as illustrated in the right column of Figure 7.

Proposed benchmark. The three proposed assessments have been used to validate the extension of CUF to multilayer functionally graded plates and to highlight the capability of some advanced models with respect to the classical ones. This allows these models to be used with confidence in order to investigate a new benchmark proposed for the first time in this paper. A three-layered plate is considered: the bottom layer is metallic made with Young's modulus $E_m = 70$ GPa and the top layer is in ceramic with $E_c = 380$ GPa. The core consists of an FGM with Young's modulus varying in z according to Zenkour's formula [2006], given here as Equation (19). The proposed plate is given in Figure 8, where the thickness of each face is $h_f = 0.1h$ and the core has $h_c = 0.8h$. In the core, the Young's modulus $E(z)$ changes exponentially in z according to an exponential parameter κ that can assume values of 1, 5 or 10, Figure 3. A fourth case has been added: a core with a constant Young's modulus, that is, an average between E_c and E_m. Poisson's ratio is constant for the three layers ($\nu = 0.3$). Two thickness ratios are investigated, $a/h = 4$ and $a/h = 100$, corresponding to $h = 0.25$ and 0.01.

Table 5 shows the displacements, Table 6 the in-plane stresses and Table 7 (on page 31) the transverse shear/normal stresses obtained. The results given by advanced models, such as LD4 and LM4, could be considered as reference values for models that will be proposed in the future by other scientists. In the case of a thick plate ($a/h = 4$), the use of LW models is mandatory, if we consider thin plates ($a/h = 100$), ESL models could be used by employing higher-order expansions. The in-plane stress σ_{xx} is considered in Figure 9, top, for κ equal to 1 and 10. Even though the plate is thick, the four theories considered are effective; an ESL model with parabolic expansion in z is enough. In the case of the transverse normal stress σ_{zz}, the use of LW models is mandatory; see Figure 9, bottom. In the case of $\kappa = 10$, the mixed model gives better values of σ_{zz} through the thickness z with respect to the LD4 theory. Some small problems have been pointed out near the top and the bottom of the plate, even though an LM4 theory is employed. This happens because the plate considered is very thick. Such problems disappear in the case of thin plates. In Figure 10, where an advanced model such as LD4 has

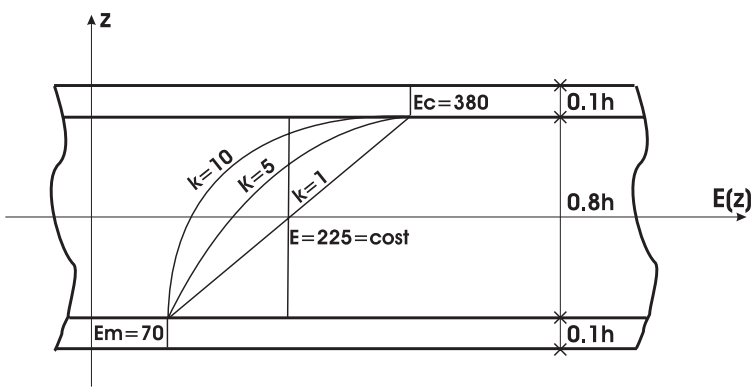

Figure 8. Benchmark: Three-layered plate with core in FGM, either obeying the law (19) proposed in [Zenkour 2006], or made of isotropic material ($E = 225$ GPa).

		$\kappa=1$		$\kappa=5$		$\kappa=10$		$E=225$ GPa	
		$\bar{w}(0)$	$\bar{u}(-2h/5)$	$\bar{w}(0)$	$\bar{u}(-2h/5)$	$\bar{w}(0)$	$\bar{u}(-2h/5)$	$\bar{w}(0)$	$\bar{u}(-2h/5)$
$a/h=4$	FSDT	0.6346	0.2084	0.8636	0.2937	0.9120	0.2969	0.5441	0.1470
	ED2	0.7520	0.2475	1.0634	0.3530	1.1143	0.3603	0.6274	0.1794
	ED4	0.7627	0.2505	1.1314	0.3504	1.2172	0.3629	0.6504	0.1844
	EMZ1	0.6655	0.2180	0.9513	0.3060	1.0554	0.3134	0.5859	0.1592
	LD4	0.7629	0.2499	1.1327	0.3530	1.2232	0.3663	0.6511	0.1852
	LM4	0.7629	0.2499	1.1329	0.3536	1.2244	0.3667	0.6511	0.1852
$a/h=100$	FSDT	0.4958	0.0083	0.6441	0.0117	0.6592	0.0119	0.4053	0.0059
	ED2	0.6073	0.0102	0.7891	0.0144	0.8075	0.0145	0.4964	0.0072
	ED4	0.6073	0.0102	0.7892	0.0144	0.8077	0.0145	0.4965	0.0072
	EMZ1	0.5083	0.0085	0.6601	0.0120	0.6801	0.0122	0.4215	0.0061
	LD4	0.6073	0.0102	0.7892	0.0144	0.8077	0.0145	0.4965	0.0072
	LM4	0.6073	0.0102	0.7892	0.0144	0.8077	0.0145	0.4965	0.0072

Table 5. Benchmark: Dimensionless normal displacement $\bar{w}=10E_ch^3u_z/(\bar{p}_za^4)$ and dimensionless in-plane displacement $\bar{u}=10E_ch^3u_x/(\bar{p}_za^4)$ for a sandwich square plate with core in FGM, using Zenkour's formula (19).

		$\kappa=1$		$\kappa=5$		$\kappa=10$		$E=225$ GPa	
		$\bar{\sigma}_{xx}(h/3)$	$\bar{\sigma}_{xy}(h/3)$	$\bar{\sigma}_{xx}(h/3)$	$\bar{\sigma}_{xy}(h/3)$	$\bar{\sigma}_{xx}(h/3)$	$\bar{\sigma}_{xy}(h/3)$	$\bar{\sigma}_{xx}(h/3)$	$\bar{\sigma}_{xy}(h/3)$
$a/h=4$	FSDT	0.6973	−0.2775	0.5003	−0.2121	0.4198	−0.1679	0.4941	−0.1976
	ED2	0.6636	−0.3094	0.4938	−0.2211	0.3872	−0.1711	0.4742	−0.2179
	ED4	0.6544	−0.3007	0.4834	−0.2022	0.3823	−0.1479	0.4663	−0.2065
	EMZ1	0.7707	−0.2551	0.6303	−0.1799	0.5309	−0.1375	0.5554	−0.1835
	LD4	0.6530	−0.3007	0.4693	−0.1999	0.3627	−0.1412	0.4801	−0.2070
	LM4	0.6531	−0.3007	0.4672	−0.1996	0.3611	−0.1403	0.4801	−0.2070
$a/h=100$	FSDT	17.344	−6.9375	13.258	−5.3033	10.495	−4.1981	12.352	−4.9408
	ED2	15.784	−8.4972	12.066	−6.4950	9.5510	−5.1413	11.241	−6.0515
	ED4	15.784	−8.4968	12.065	−6.4943	9.5509	−5.1404	11.241	−6.0511
	EMZ1	18.928	−7.1107	15.244	−5.4326	12.597	−4.3287	13.554	−5.1375
	LD4	15.784	−8.4968	12.065	−6.4942	9.5501	−5.1402	11.242	−6.0511
	LM4	15.784	−8.4968	12.065	−6.4942	9.5500	−5.1401	11.242	−6.0511

Table 6. Benchmark: Dimensionless in-plane stresses $\bar{\sigma}_{xx}=h\sigma_{xx}/(a\bar{p}_z)$ and $\bar{\sigma}_{xy}=h\sigma_{xy}/(a\bar{p}_z)$ for a sandwich square plate with core in FGM, using Zenkour's formula (19).

been chosen, the displacements and the stresses are investigated in the thickness z direction for the case of four different cores ($\kappa=1$, $\kappa=5$, $\kappa=10$, and $E_c=\text{constant}=225$ GPa) and for the thickness ratio $a/h=10$. The displacements in the z direction obtained using a core with a constant Young's modulus

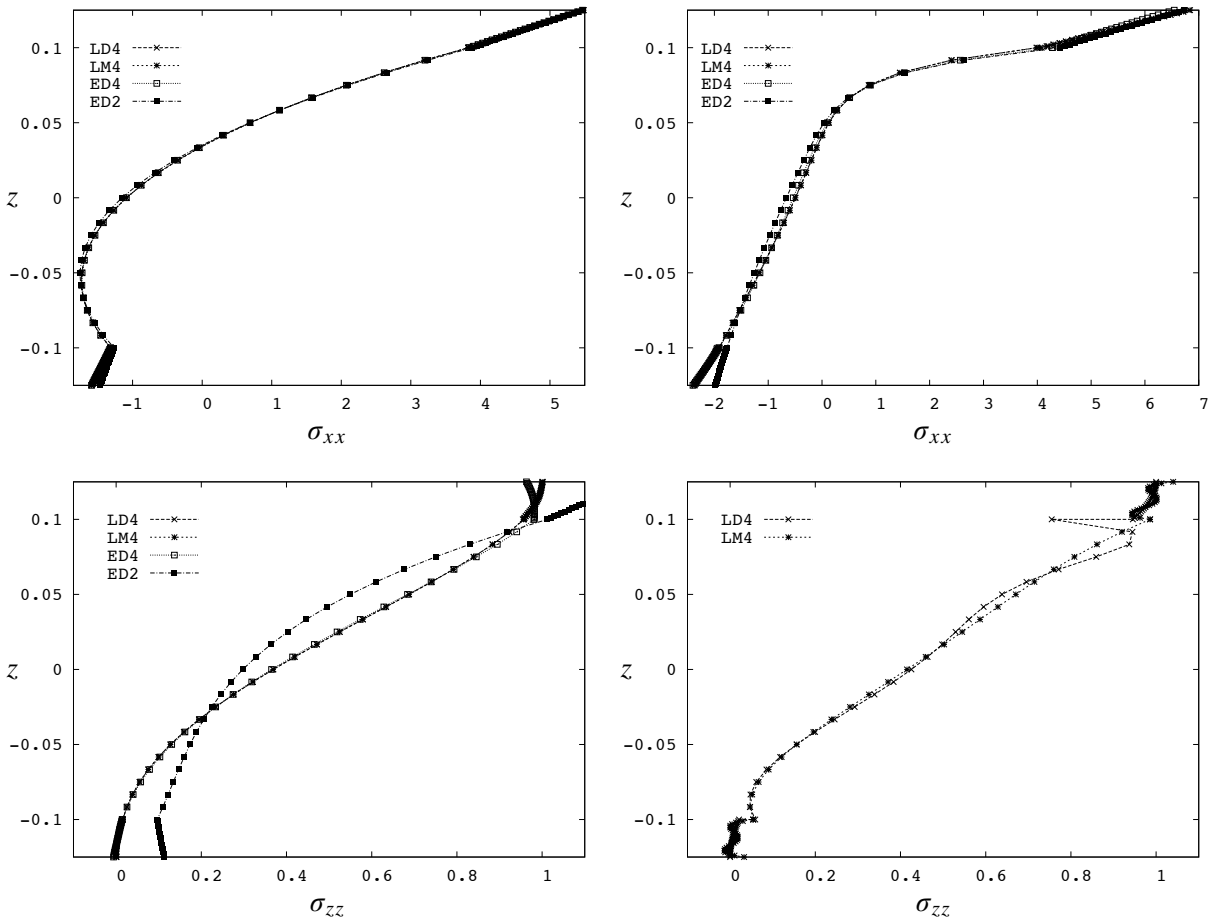

Figure 9. Benchmark: Sandwich plate with core in FGM. In-plane stress σ_{xx} (top row) and transverse-normal stress σ_{zz} (bottom row) versus z for $\kappa = 1$ (left) and $\kappa = 10$ (right). The thickness ratio is $a/h = 4$.

are more conservative than the FGM core cases (top row in Figure 10). On the contrary, the use of an FGM core allows in-plane stresses σ_{xx} and σ_{xy} continuous in the z direction to be obtained, which is not possible with a "classical" core, and the typical discontinuity of in-plane stresses for the sandwich structures is clearly shown (middle row in Figure 10). The discontinuity exhibited by the FGM core in the case of transverse shear and normal stresses σ_{xz} and σ_{zz} in Figure 10 is due to the use of a PVD model. These stresses can actually be obtained continuously in z if we use a mixed model, as already seen in Figure 7.

5. Conclusions

This paper has investigated the static response of several sandwich plates that include different types of functionally graded layers. Conclusions have been outlined, regarding the modeling tools used for these types of structure and the design of sandwich plates including a core in FGM. It has been shown

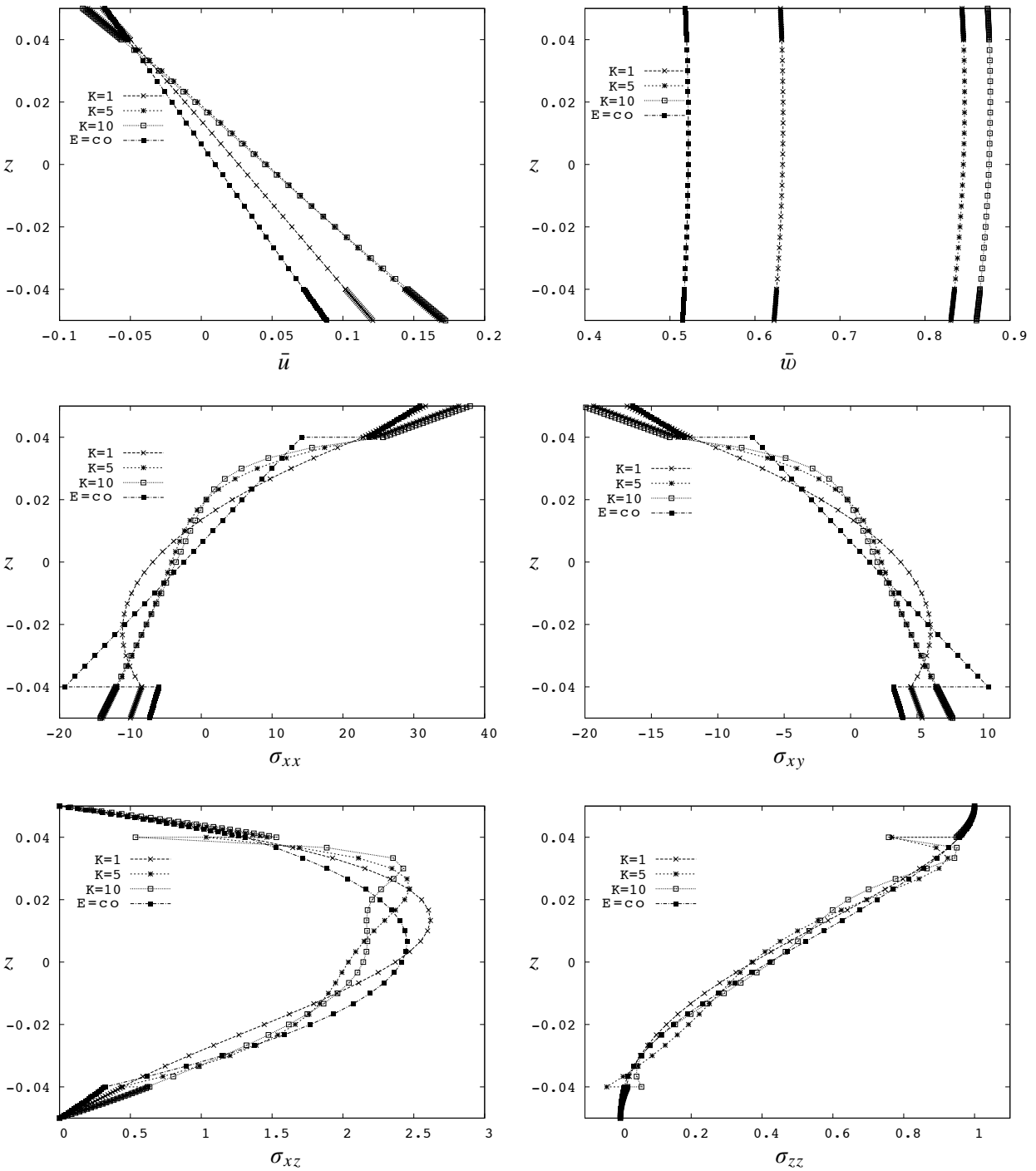

Figure 10. Benchmark: For the sandwich plate with core in FGM, displacements $(\bar{u}, \bar{w}) = 10(u_x, u_z)E_c h^3/(\bar{p}_z a^4)$ and stresses σ_{xx}, σ_{xy}, σ_{xz} and σ_{zz} versus z for LD4 theory. In addition to the values $\kappa = 1, 5, 10$ in Zenkour's formula (19), we consider an isotropic material with $E = 225$ GPa for the core ("E = co"). Thickness ratio: $a/h = 10$.

		$\kappa = 1$		$\kappa = 5$		$\kappa = 10$		$E = 225\,\text{GPa}$	
		$\bar{\sigma}_{xz}(0)$	$\bar{\sigma}_{zz}(0)$	$\bar{\sigma}_{xz}(0)$	$\bar{\sigma}_{zz}(0)$	$\bar{\sigma}_{xz}(0)$	$\bar{\sigma}_{zz}(0)$	$\bar{\sigma}_{xz}(0)$	$\bar{\sigma}_{zz}(0)$
$a/h = 4$	FSDT	0.1591	−0.1811	0.0891	−0.1113	0.0906	−0.0965	0.1591	−0.0677
	ED2	0.1913	0.0743	0.1205	0.0429	0.1177	0.0453	0.1704	0.0959
	ED4	0.2374	0.0912	0.1925	0.0833	0.2015	0.0970	0.2400	0.1157
	EMZ1	0.1923	−0.0002	0.1327	0.0051	0.1409	0.0403	0.1950	0.1272
	LD4	0.2345	0.0922	0.1998	0.0911	0.2113	0.1064	0.2405	0.1058
	LM4	0.2345	0.0922	0.2026	0.0924	0.2124	0.1067	0.2403	0.1058
$a/h = 100$	FSDT	0.1591	−4.5270	0.0891	−2.7824	0.0906	−2.4115	0.1591	−1.6935
	ED2	0.1945	0.0084	0.1225	0.0018	0.1192	0.0019	0.1726	0.0039
	ED4	0.2403	0.0037	0.1965	0.0034	0.2043	0.0039	0.2415	0.0046
	EMZ1	0.1950	−2.7104	0.1350	−1.6383	0.1378	−1.2957	0.1955	−0.1044
	LD4	0.2375	0.0038	0.2046	0.0037	0.2149	0.0043	0.2417	0.0042
	LM4	0.2375	0.0038	0.2055	0.0037	0.2122	0.0042	0.2417	0.0042

Table 7. Benchmark: Dimensionless transverse shear stress $\bar{\sigma}_{xz} = h\sigma_{xz}/(a\bar{p}_z)$ and transverse normal stress $\bar{\sigma}_{zz} = h\sigma_{zz}/(a\bar{p}_z)$ for a sandwich square plate with core in FGM, using Zenkour's formula (19).

that in order to investigate multilayer plates embedding FGM layers, the use of advanced models is mandatory, in particular for thick and moderately thick plates as well as for complicated laws in the z direction given for the material properties. To obtain a quasi-three-dimensional response, LW models and high orders of expansion are necessary. Mixed models are convenient for particular variables such as transverse shear/normal stresses. In the design of sandwich plates, the use of FGM cores can represent a valid alternative to classical materials, because they allow particular features, such as the continuity of in-plane stresses in the thickness direction, that conventional cores do not allow. The discussion about the optimum design of multilayer plates including FGM layers could be the subject of future works. In them the heat conduction problem will be considered and material properties will be dependent on temperature.

References

[Anderson 2003] T. A. Anderson, "A 3-D elasticity solution for a sandwich composite with functionally graded core subjected to transverse loading by a rigid sphere", *Compos. Struct.* **60**:3 (2003), 265–274.

[/'Avila 2007] A. F. /'Avila, "Failure mode investigation of sandwich beams with functionally graded core", *Compos. Struct.* **81**:3 (2007), 323–330.

[Batra and Jin 2005] R. C. Batra and J. Jin, "Natural frequencies of a functionally graded anisotropic rectangular plate", *J. Sound Vib.* **282**:2 (2005), 509–516.

[Birman and Byrd 2007] V. Birman and L. W. Byrd, "Modeling and analysis of functionally graded materials and structures", *Appl. Mech. Rev.* **60**:5 (2007), 195–216.

[Brischetto and Carrera 2008] S. Brischetto and E. Carrera, "Advanced mixed theories for bending analysis of functionally graded plates", *Comput. Struct.* (2008). In press.

[Carrera 1995] E. Carrera, "A class of two-dimensional theories for anisotropic multilayered plates analysis", *Mem. Accad. Sci. Torino Cl. Sci. Fis. Mat. Natur.* **19–20** (1995), 49–87.

[Carrera 2002] E. Carrera, "Theories and finite elements for multilayered, anisotropic, composite plates and shells", *Arch. Comput. Methods Eng.* **9**:2 (2002), 87–140.

[Carrera 2003] E. Carrera, "Historical review of zig-zag theories for multilayered plates and shells", *Appl. Mech. Rev.* **56**:3 (2003), 287–308.

[Carrera and Brischetto 2008] E. Carrera and S. Brischetto, "Analysis of thickness locking in classical, refined and mixed multilayered plate theories", *Compos. Struct.* **82**:4 (2008), 549–562.

[Carrera et al. 2008] E. Carrera, S. Brischetto, and A. Robaldo, "Variable kinematic model for the analysis of functionally graded material plates", *AIAA J.* **46**:1 (2008), 194–203.

[Cauchy 1828] A. L. Cauchy, "Sur l'équilibre et le mouvement d'une plaque solide", pp. 381–411 in *Œuvres complètes d'Augustin Cauchy: exercices de mathématique (anciens exercices)*, vol. 8, Ser. 2, Gauthier-Villars, Paris, 1828.

[Cheng and Zhong 2007] Z. Cheng and Z. Zhong, "Analysis of a moving crack in a functionally graded strip between two homogeneous layers", *Int. J. Mech. Sci.* **49**:9 (2007), 1038–1046.

[Chi and Chung 2006] S.-H. Chi and Y.-L. Chung, "Mechanical behavior of functionally graded material plates under transverse load, I: Analysis", *Int. J. Solids Struct.* **43**:13 (2006), 3657–3674.

[Dahan et al. 2001] I. Dahan, U. Admon, N. Frage, J. Sariel, M. P. Dariel, and J. J. Moore, "The development of a functionally graded TiC-Ti multilayer hard coating", *Surf. Coat. Technol.* **137**:2–3 (2001), 111–115.

[Etemadi et al. 2008] E. Etemadi, A. Afaghi-Khatibi, and M. Takaffoli, "3D finite element simulation of sandwich panels with a functionally graded core subjected to low velocity impact", *Compos. Struct.* (2008). In press.

[Ferreira et al. 2005] A. J. M. Ferreira, R. C. Batra, C. M. C. Roque, L. F. Qian, and P. A. L. S. Martins, "Static analysis of functionally graded plates using third-order shear deformation theory and a meshless method", *Compos. Struct.* **69**:4 (2005), 449–457.

[Kashtalyan 2004] M. Kashtalyan, "Three-dimensional elasticity solution for bending of functionally graded rectangular plates", *Eur. J. Mech. A Solids* **23**:5 (2004), 853–864
.

[Kashtalyan and Menshykova 2009] M. Kashtalyan and M. Menshykova, "Three-dimensional elasticity solution for sandwich panels with a functionally graded core", *Compos. Struct.* **87**:1 (2009), 36–43.

[Kirchhoff 1850] G. Kirchhoff, "Über das Gleichgewicht und die Bewegung einer elastischen Scheibe", *J. Reine Angew. Math.* **40** (1850), 51–88.

[Kirugulige et al. 2005] M. S. Kirugulige, R. Kitey, and H. V. Tippur, "Dynamic fracture behavior of model sandwich structures with functionally graded core: a feasibility study", *Compos. Sci. Technol.* **65**:7–8 (2005), 1052–1068.

[Li and Fan 2007] X.-F. Li and T.-Y. Fan, "Dynamic analysis of a crack in a functionally graded material sandwiched between two elastic layers under anti-plane loading", *Compos. Struct.* **79**:2 (2007), 211–219.

[Li et al. 2008] Q. Li, V. P. Iu, and K. P. Kou, "Three-dimensional vibration analysis of functionally graded material sandwich plates", *J. Sound Vib.* **311**:1–2 (2008), 498–515.

[Mindlin 1951] R. D. Mindlin, "Influence of rotatory inertia and shear in flexural motions of isotropic elastic plates", *J. Appl. Mech.* (*ASME*) **18** (1951), 31–28.

[Mori and Tanaka 1973] T. Mori and K. Tanaka, "Average stress in matrix and average elastic energy of materials with misfitting inclusions", *Acta Metall.* **21**:5 (1973), 571–574.

[Murakami 1986] H. Murakami, "Laminated composite plate theory with improved in-plane responses", *J. Appl. Mech.* (*ASME*) **53** (1986), 661–666.

[Nguyen et al. 2008] T.-K. Nguyen, K. Sab, and G. Bonnet, "First-order shear deformation plate models for functionally graded materials", *Compos. Struct.* **83**:1 (2008), 25–36.

[Poisson 1829] S. D. Poisson, "Mémoire sur l'équilibre et le mouvement des corps élastiques", *Mém. Acad. Sci. Paris* **8** (1829), 357–570.

[Qian et al. 2004] L. F. Qian, R. C. Batra, and L. M. Chen, "Static and dynamic deformations of thick functionally graded elastic plates by using higher-order shear and normal deformable plate theory and meshless local Petrov–Galerkin method", *Compos. B Eng.* **35**:6–8 (2004), 685–697.

[Ramirez et al. 2006] F. Ramirez, P. R. Heyliger, and E. Pan, "Static analysis of functionally graded elastic anisotropic plates using a discrete layer approach", *Compos. B Eng.* **37**:1 (2006), 10–20.

[Reddy 2004] J. N. Reddy, *Mechanics of laminated composite plates: theory and analysis*, CRC Press, New York, 2004.

[Reddy and Cheng 2001] J. N. Reddy and Z.-Q. Cheng, "Three-dimensional thermomechanical deformations of functionally graded rectangular plates", *Eur. J. Mech. A Solids* **20**:5 (2001), 841–855.

[Reissner 1945] E. Reissner, "The effect of transverse shear deformation on the bending of elastic plates", *J. Appl. Mech.* (*ASME*) **12** (1945), A–69–A–77.

[Reissner 1984] E. Reissner, "On a certain mixed variational theorem and a proposed application", *Int. J. Numer. Methods Eng.* **20**:7 (1984), 1366–1368.

[Shen and Li 2008] H.-S. Shen and S.-R. Li, "Postbuckling of sandwich plates with FGM face sheets and temperature-dependent properties", *Compos. B Eng.* **39**:2 (2008), 332–344.

[Shodja et al. 2007] H. M. Shodja, H. Haftbaradaran, and M. Asghari, "A thermoelasticity solution of sandwich structures with functionally graded coating", *Compos. Sci. Technol.* **67**:6 (2007), 1073–1080.

[Vel and Batra 2002] S. S. Vel and R. C. Batra, "Exact solution for thermoelastic deformations of functionally graded thick rectangular plates", *AIAA J.* **40**:7 (2002), 1421–1433.

[Vel and Batra 2003] S. S. Vel and R. C. Batra, "Three-dimensional analysis of transient thermal stresses in functionally graded plates", *Int. J. Solids Struct.* **40**:25 (2003), 7181–7196.

[Vel and Batra 2004] S. S. Vel and R. C. Batra, "Three-dimensional exact solution for the vibration of functionally graded rectangular plates", *J. Sound Vib.* **272**:3–5 (2004), 703–730.

[Xia and Shen 2008] X.-K. Xia and H.-S. Shen, "Vibration of post-buckled sandwich plates with FGM face sheets in a thermal environment", *J. Sound Vib.* **314**:1–2 (2008), 254–274.

[Zenkour 2005a] A. M. Zenkour, "A comprehensive analysis of functionally graded sandwich plates, 1: Deflection and stresses", *Int. J. Solids Struct.* **42**:18–19 (2005), 5224–5242.

[Zenkour 2005b] A. M. Zenkour, "A comprehensive analysis of functionally graded sandwich plates, 2: Buckling and free vibration", *Int. J. Solids Struct.* **42**:18–19 (2005), 5243–5258.

[Zenkour 2006] A. M. Zenkour, "Generalized shear deformation theory for bending analysis of functionally graded plates", *Appl. Math. Model.* **30**:1 (2006), 67–84.

[Zhao et al. 2008] J. Zhao, Y. Li, and X. Ai, "Analysis of transient thermal stress in sandwich plate with functionally graded coatings", *Thin Solid Films* **516**:21 (2008), 7581–7587.

[Zhu and Sankar 2007] H. Zhu and B. V. Sankar, "Analysis of sandwich TPS panel with functionally graded foam core by Galerkin method", *Compos. Struct.* **77**:3 (2007), 280–287.

Received 11 Jul 2008. Revised 27 Oct 2008. Accepted 1 Nov 2008.

SALVATORE BRISCHETTO: salvatore.brischetto@polito.it
Politecnico di Torino, Department of Aeronautics and Space Engineering, Corso Duca Degli Abruzzi, 24, 10129 Torino, Italy